Dalton Transactions

The effect of ligand symmetry on the ratiometric luminescence characteristics of lanthanides

Journal:	*Dalton Transactions*
Manuscript ID	DT-ART-03-2018-000898.R2
Article Type:	Paper
Date Submitted by the Author:	11-Apr-2018
Complete List of Authors:	Okayasu, Yoshinori; Tokyo Koka Daigaku, Applied Sciences Kamebuchi, Hajime; Tokyo University of Science, Faculty of Science, Department of Chemistry Yuasa, Junpei; Tokyo University of Science, Deapartment of Applied Chemistry

Dalton Transactions

ARTICLE

The effect of ligand symmetry on the ratiometric luminescence characteristics of lanthanides

Yoshinori Okayasu[a] Hajime Kamebuchi[b] and Junpei Yuasa*[a,c]

Received 00th January 20xx,
Accepted 00th January 20xx

DOI: 10.1039/x0xx00000x

www.rsc.org/

This work demonstrated that the ligand symmetry of europium(III) complexes controls the ratiometric luminescence characteristics of the lanthanide. Nona-coordinated europium(III) complexes having unsymmetrical β-diketonate ligands (C_s) exhibit distinctive ratiometric spectral variations in the extremely narrow *f-f* transition bands over the temperature range 253 to 323 K. Conversely, no such ratiometric change can be observed in a series of nona-coordinated europium(III) complexes containing symmetrical β-diketonate ligands (C_{2v}). The remarkable difference depending on the ligand symmetry (C_s vs C_{2v}) suugests that coordination rearrenegment of the β-diketonate in the complex causes the ratiometric spectral variations in the extremely narrow *f-f* transition bands, where two europium(III) complex isomers exist in the solution equilibrium. A self-calibration method using dual iso-emissive points is reported, where self-calibration using the two emission intensities at the iso-emissive points reduces the coefficient of variation in the luminensece thermometry.

Introduction

Symmetry is a fundamental concept in coordination chemistry, as it can explain the optical properties of metal complexes. Crystal-field symmetry has an especially large effect on the optical properties of lanthanides. As an example, low crystal-field symmetry results in splitting of the ^7F_J levels of Eu^{3+}, such that the line-type emission of Eu^{3+} is further split based on crystal field levels.[1,2] Changes in the crystal field symmetry will modulate the relative intensities of these lines, with significant variations in the profile of the narrow crystal field transition lines (within a few 10^2 cm^{-1}) with respect to changes in a parameter of interest.[3,4] These intrinsic characteristics of the lanthanides may allow high resolution, highly accurate ratiometric measurements.[4] This represents a useful complementary approach to the mixed lanthanide strategy based on employing the dual luminescent intensities from two different lanthanide ions (e.g., Eu^{3+}/Tb^{3+}).[5–11] As a result, there has been extensive development of lanthanide-based ratiometric sensing systems over the last decade.[12–15] Despite this progress, variations in ratiometric emissions resulting from crystal-field alternations are difficult to predict, because these changes generally stem from modifications of the crystal-field symmetry of coordinatively unsaturated complexes.[4] Thus, a general platform for the design of lanthanide-based ratiometric systems would significantly expand the scope of sensor technologies.

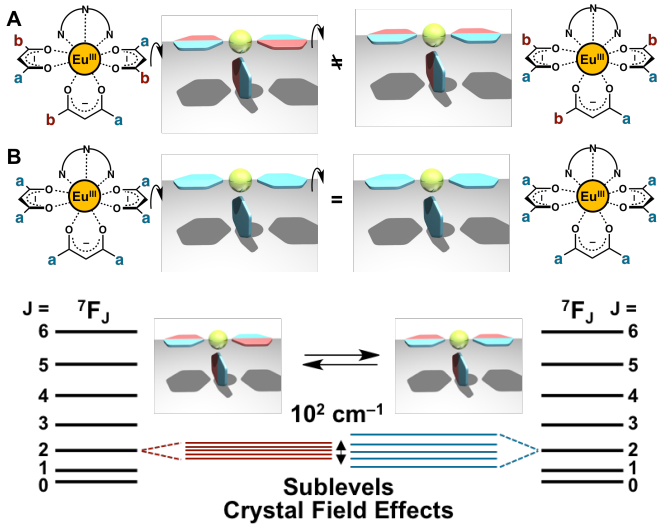

Scheme 1. Top: nona-coordinated Eu^{3+} complexes incorporating (A) a tridentate ligand with unsymmetrical β-diketonate ligands, and (B) a tridentate ligand with symmetrical β-diketonate ligands. Rotation arrows indicate coordination-rearrangement of the β-diketonate ligands. Bottom: a partial energy diagram of Eu^{3+} (^7F_J) showing the relative magnitude of the crystal-field effects (sublevels) of nona-coordinated Eu^{3+} complexes.

Herein, we present a general strategy for lanthanide-based ratiometric sensing systems based on the intrinsic ratiometric characteristics associated with lanthanide luminescence. This work demonstrates that the ligand symmetry of nona-coordinated europium(III) complexes affects the ratiometric luminescence characteristics of the lanthanide. A series of nona-coordinated complexes was designed having a combination of a

[a] Department of Applied Chemistry, Tokyo University of Science, Kagurazaka, Shinjuku, Tokyo 162-8601, Japan. E-mail: yuasaj@rs.tus.ac.jp
[b] Department of Chemistry, Tokyo University of Science, Kagurazaka, Shinjuku, Tokyo 162-8601, Japan.
[c] Precursory Research for Embryonic Science and Technology (PRESTO), Science and Technology Agency (JST), 4-1-8 Honcho, Kawaguchi, Saitama 332-0012, Japan.

† Electronic Supplementary Information (ESI) available: Additional experimental details and additional spectral crystallographic data. CCDC 1834910. For ESI and crystallographic data in CIF or other electronic format See DOI: 10.1039/x0xx00000x

tridentate ligand and three β-diketonate ligands (C_s and C_{2v}) to give coordinatively saturated lanthanide complexes.[16–18] This series of complexes can be divided into two groups depending on the symmetry of the β-diketonate ligands: (A) nona-coordinated complexes having a tridentate ligand with three unsymmetrical β-diketonate ligands (C_{2s}) and (B) those comprised of a tridentate ligand with three symmetrical β-diketonate ligands (C_{2v}). Coordination-rearrangement of the unsymmetrical β-diketonate ligand results in the isomerization of the nona-coordinated structure (Scheme 1A). These isomeric coordination geometries can reversibly interconvert through a relatively flat potential energy surface due to the labile character of the lanthanide ions, which results in crystal-field alternation with a dramatic change in the line-type emission profile of the *f*-*f* transition at the crystal-field sublevels (Scheme 1, bottom). Conversely, coordination-rearrangement of the symmetrical β-diketonate ligand does not result in coordination isomerization (Scheme 1B), hence these complexes serve as reference compounds to validate the above concept. In the present work, ratiometric temperature sensing was demonstrated, as temperature is the most important and the frequently measured physical property.[4,19–27] A new self-calibration method using dual iso-emissive points is also reported.

Results and discussion

We systematically investigated nona-coordinated Eu^{3+} complexes with various ligand symmetries based on tridentate ligands (C_s, C_2, and C_{2v}) and β-diketonate ligands (C_s and C_{2v}) to establish the feasibility of this strategy (**1**–**8**, see the structures in Figs. 1 and 2). In each case, the Eu^{3+} complex in acetonitrile generates sharp emission peaks due to *f*-*f* transitions of the Eu^{3+} ions ($^5D_0 \rightarrow {}^7F_J$, J = 0–4), and the intensity of the emission peaks decrease with increases in the temperature from 253 to 323 K (Fig. 1). This effect can likely be attributed to enhancement of the back energy transfer processes at higher temperatures, which is a well-known process responsible for the emission quenching of Eu^{3+} complexes having β-diketonate antenna ligands.[28] Interestingly, when the emission spectra are normalized to the emission intensity for the $^5D_0 \rightarrow {}^7F_1$ transition band (λ = 591 nm), the nona-coordinated Eu^{3+} complexes having unsymmetrical β-diketonate ligands (**1**–**5**) all exhibit clear iso-emission points in the $^5D_0 \rightarrow {}^7F_2$ and $^5D_0 \rightarrow {}^7F_4$ transition bands (Figs. 2a–e and Table 1). The $^5D_0 \rightarrow {}^7F_1$ transition is relatively insensitive to the ligand field of the Eu^{3+} while the $^5D_0 \rightarrow {}^7F_2$ transition is sensitive to the crystal-field symmetry around the Eu^{3+} ions. Hence, the ratio of the $^5D_0 \rightarrow {}^7F_2$ to $^5D_0 \rightarrow {}^7F_1$ emission intensities often reflects changes in the crystal-field symmetry of nona-coordinated Eu^{3+} complexes.[4] In the present case, the iso-emissive points associated with the ratiometric emission spectral changes of **1**–**5** (Figs. 2a–e) suggest a transformation between the two nona-coordinated geometries in response to temperature changes (Scheme 1). The typical ratiometric performance of **1** for temperature sensing is shown in Fig. 3a, where the normalized emission intensities at λ = 612 and 620 nm change from 15.4 to 27.7 and from 15.7 to 12.2, respectively, with the increase in temperature. This process is found to be fully reversible based on repeated cycles between 253 and 323 K (Fig. 3a). Conversely, there is

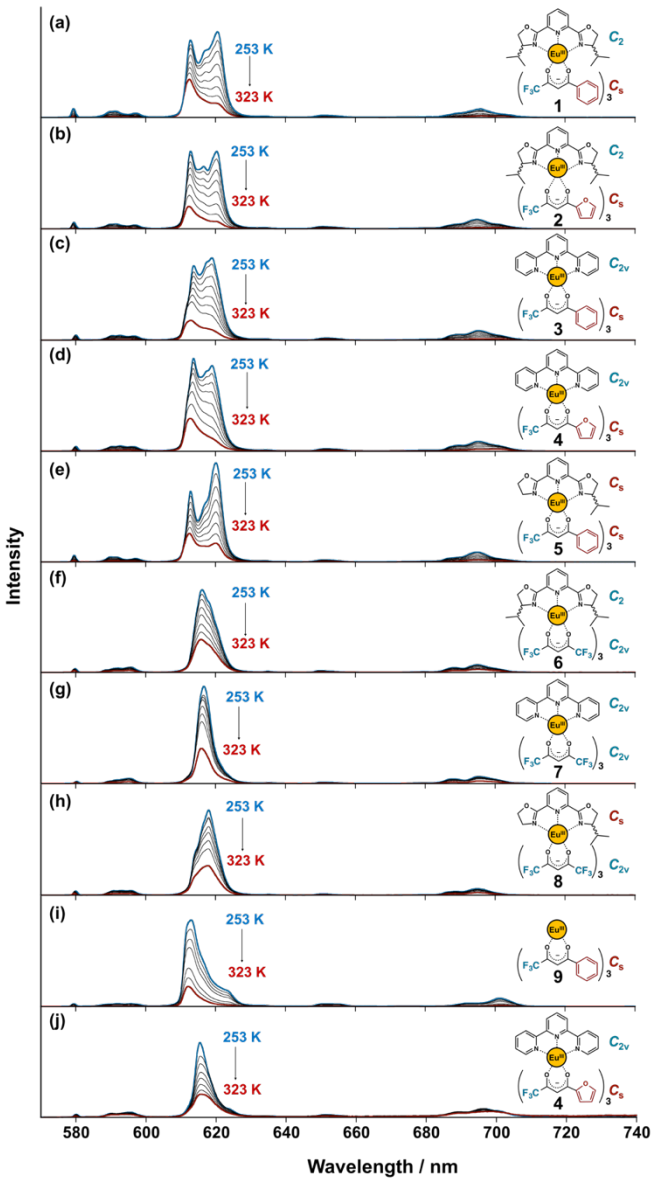

Fig 1. (a)–(i) Non-normalized emission spectra of **1**–**9** (1.0×10^{-5} M) in acetonitrile at 253–323 K. (j) Solid-state (KBr pellet) emission spectra of **4** at 253–323 K. Excitation wavelength: (a) and (d)–(h) λ_{ex} = 330 nm, (b) λ_{ex} = 320 nm, and (c) λ_{ex} = 340 nm.

Table 1 Combinations of ligand symmetry and the resulting ratiometric responses to temperature changes

	Tridentate ligand symmetry		
	C_S	C_2	C_{2v}
Unsymmetrical β-diketonate (C_s)	+	+	+
Symmetrical β-diketonate (C_{2v})	–	–	–

no intensity change during such cycles at the iso-emissive points (λ = 617 and 598 nm, Fig 2a, filled circles). This ratiometric behavior is interesting because it enables self-calibration using dual iso-emissive points. Therefore, as a primitive trial, the normalized emission intensity at λ = 612 nm (I_{612}/I_{591}) was further calibrated using the intensity difference between the two iso-emissive points ($I_{617} - I_{598}$). The accuracy of temperature sensing during the temperature change

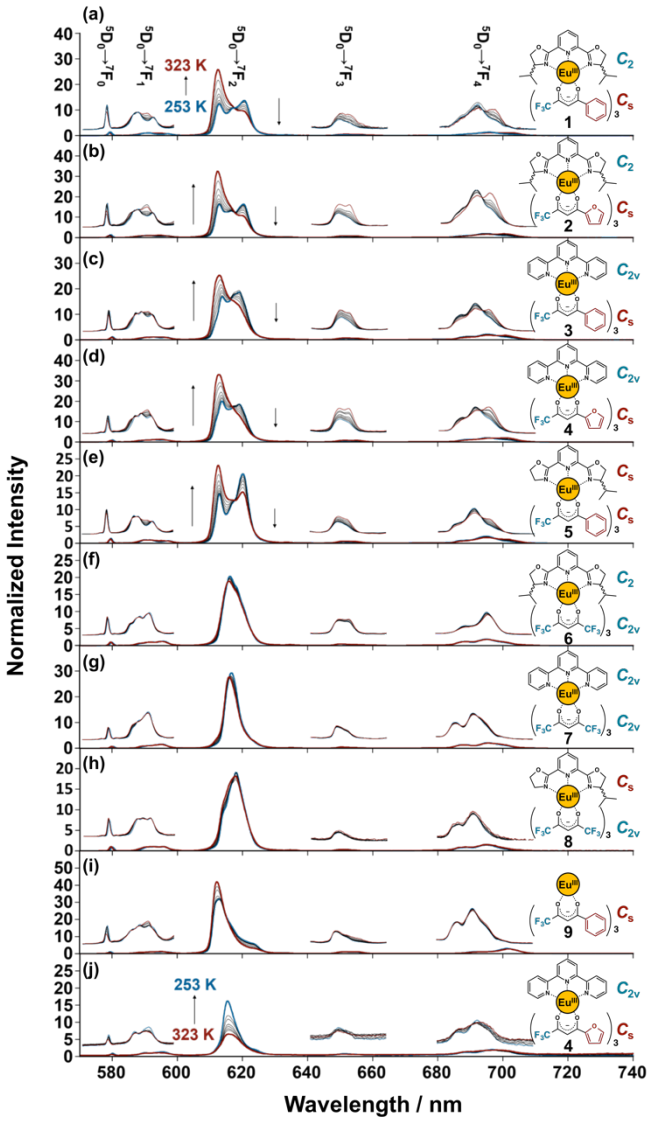

Fig 2. (a)–(i) Emission spectra of **1**–**9** (1.0×10^{-5} M) in acetonitrile at 253–323 K. (j) Solid state (KBr pellet) emission spectra of **4** at 253–323 K. Spectra are normalized to the emission intensity at $\lambda = 591$ nm. Excitation wavelengths: (a) and (d)–(h) $\lambda_{ex} = 330$ nm, (b) $\lambda_{ex} = 320$ nm, and (c) $\lambda_{ex} = 340$ nm. Insets: emission intensities for the $^5D_0 \rightarrow {}^7F_0$, $^5D_0 \rightarrow {}^7F_1$, $^5D_0 \rightarrow {}^7F_3$ and $^5D_0 \rightarrow {}^7F_4$ transition bands are enlarged and the chemical structures of **1**–**9** are shown, where C_s, C_2 and C_{2v} indicate ligand symmetry.

$$(CV)^2 = \frac{1}{(N-1)} \sum_{i=1}^{N} (x_i/m - 1)^2 \qquad (1)$$

cycle is subsequently assessed based on the coefficient of variation (*CV*) at each temperature (Fig. 3b). Eqn (1) represents the definition of *CV*, where *N* denotes the number of data points, x_i indicates the measured values, and *m* shows the average values. The calibrated values ($(I_{612}/I_{591})/(I_{617} - I_{598})$) show a better (that is, lower) *CV* at each temperature. As an example, a *CV* of 0.99 was obtained for the calibrated values, compared to 1.62 for the non-calibrated values (I_{612}/I_{591}), at 283 K. The lower *CV* in this case indicates the validity of calibration using dual iso-emissive points.

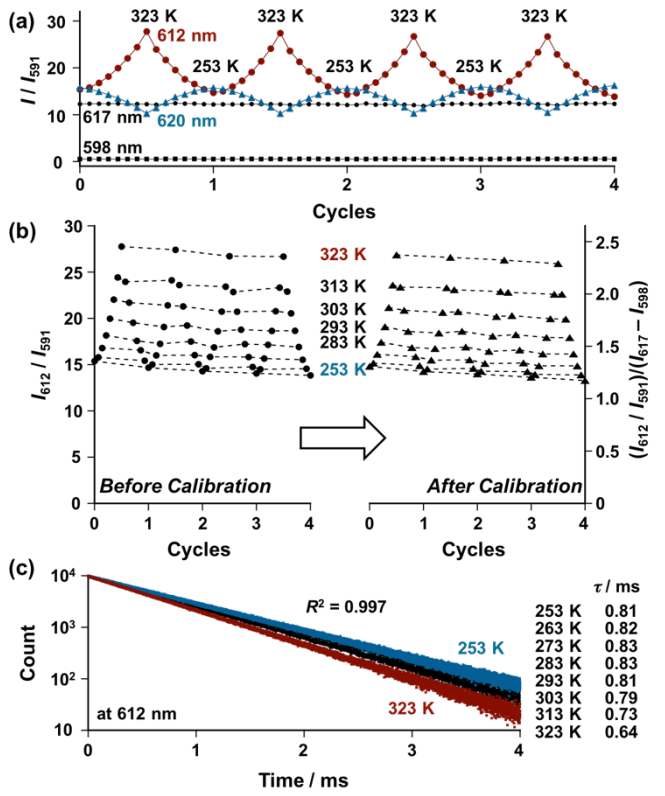

Fig 3. (a) Normalized emission intensity values (I/I_{591}) of **1** (1.0×10^{-5} M) at λ = 612 nm (red circles), 620 nm (blue triangles), 617 nm (black circles) and 598 nm (black squares) in acetonitrile at 253–323 K. (b) Normalized emission intensity values at $\lambda = 612$ nm before calibration (I_{612}/I_{591}) and after calibration [$(I_{612}/I_{591})/(I_{617} - I_{598})$] at 253–323 K. (c) Emission decay profiles of **1** (1.0×10^{-5} M) at $\lambda = 612$ nm in acetonitrile at 253–323 K.

In contrast to the Eu^{3+} complexes having the unsymmetrical *β*-diketonate ligands (**1**–**5**), those incorporating symmetrical *β*-diketonate ligands (**6**–**8**) show no ratiometric response to temperature changes. As such, no appreciable spectral changes were observed over each temperature range (Figs. 2e–h and Table 1). Similarly, an unsymmetrical tris-*β*-diketonate Eu^{3+}complex without a tridentate ligand (**9**) did not exhibit any spectral shape changes as a function of temperature (Fig. 1i). These negative results suggest that each of the reference complexes **6**–**9** exists as a single emitting species over the temperature range of 253 to 323 K. There is no possible isomerization or coordination-rearrangement around the Eu^{3+} in **6**–**8**, all of which have symmetrical *β*-diketonate ligands (*vide supra*, Scheme 1B). Conversely, coordination-rearrangement of the unsymmetrical *β*-diketonate ligand around the Eu^{3+} center provides the opportunity for coordination isomerization in **1**–**5** (*vide supra*, Scheme 1A). Thus, the negative control experiments (Figs. 2e–i and Table 1) provide convincing evidence that coordination-rearrangement of the unsymmetrical *β*-diketonate ligands in **1**–**5** leads to isomerization of the nona-coordination geometries based on a temperature-dependent equilibrium (*vide supra*, Scheme 1 bottom).

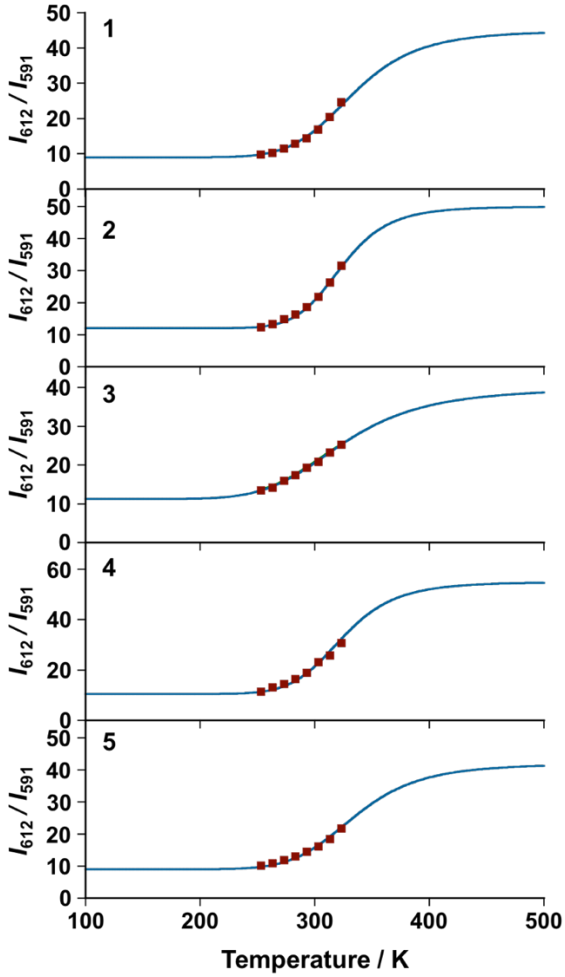

Fig 4. Temperature dependence of emission intensities (I_{612}) of **1**–**5** (1.0×10^{-5} M) at 612 nm in acetonitrile at 253–323 K. The solid line shows a fitting curve using eqn (2).

Table 2 Thermodynamic parameters for the transition between the two coordination isomers of **1**–**5** in acetonitrile

	Complex				
	1	**2**	**3**	**4**	**5**
ΔH^0 (kJ mol^{-1})	32.7	41.8	29.2	37.6	32.3
ΔS^0 (J mol^{-1} K^{-1})	98.0	126	82.0	116	96.4

Assuming a two-state equilibrium,[4,29] the ratiometric emission changes of **1**–**5** as a function of temperature (Figs. 2a–e) can be expressed by eqn (2), where ΔH^0 and ΔS^0 respectively denote the

$$I = \{I_0 + I_\infty \exp(-\Delta H^0/RT + \Delta S^0/R)\}/\{1 + \exp(-\Delta H^0/RT + \Delta S^0/R)\} \quad (2)$$

enthalpy and entropy changes on going between the two isomeric coordination geometries, and I_0 and I_∞ represent their normalized emission intensities. The ΔH^0 and ΔS^0 values in Table 2 were determined by fitting the intensity changes (I) at 612 nm with eqn (2) (Fig. 4). Relatively small ΔH^0 values (29–42 kJ mol^{-1}) are found for **1**–**5** in each case, suggesting similar thermodynamic stabilities between the two isomeric nona-coordinated geometries. This small enthalpy change may correspond to a difference between the two coordination isomers in terms of intra-complex ligand-ligand interactions and/or solvent-complex interactions. In contrast, the relatively large entropy changes (ΔS^0 = 82–126 J mol^{-1} K^{-1}) suggest a higher degree of freedom for the solvent molecules surrounding the complexes at higher temperatures.

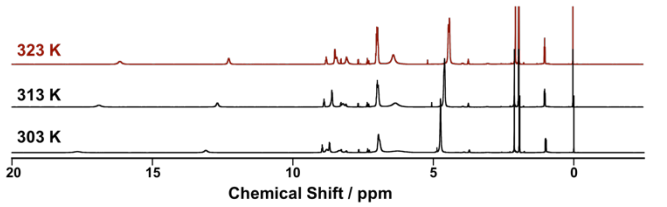

Fig 5. ^{1}H NMR spectra of **1** in CD_3CN at 303, 313 and 323 K.

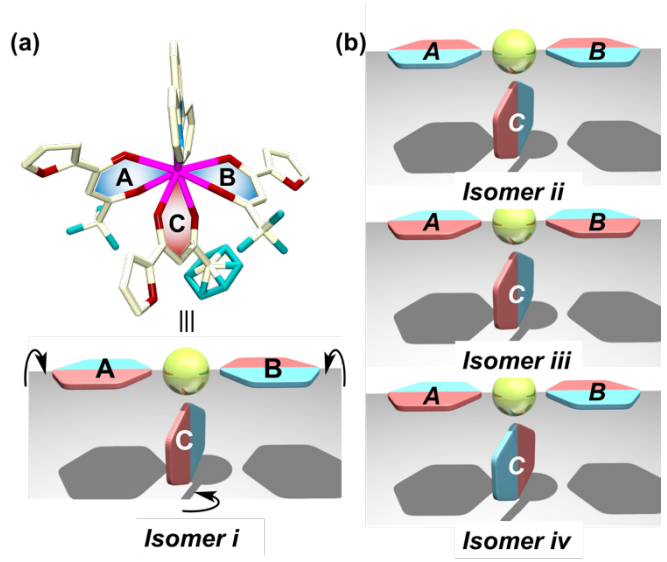

Fig 6. (a) Top: X-ray crystal structure of **4** (CCDC 1834910). Hydrogen atoms and solvent molecules are omitted for clarity. Bottom: schematic representation of the coordination geometry of the three unsymmetrical β-diketonate ligands around Eu^{3+}. Rotation arrows indicate coordination-rearrangement of the β-diketonate ligands. (b) Possible coordination isomers of **4**.

To verify the emissive species, emission lifetime measurements of **1** were conducted over the temperature range of 253 to 323 K (Fig. 3c). However, contrary to our expectations, the emission of **1** exhibits a single-exponential decay at each temperature (Fig. 3c). We measured the long-lived emission from the Eu^{III} complex in the Multi Chanel Scale (MCS) mode. In such a case, a delay is implemented between the excitation pulse and the signal is integrated during a time called gate time, hence there is a possibility that the measured lifetime is simply an average value of the excited state lifetimes of the two (or more isomers) if the gate time is long enough (few milliseconds) compared to the inverse of the rate of exchange between the isomers.

Then, we performed the various temperature (VT) NMR of **1** over the range of 303–323 K, where **1** showed NMR peak shifts with increasing in temperature, in agreement with the equilibrium shifts between the complexes. No apparent complex decomposition is observed in the NMR spectra in this temperature range (Fig. 5).[30] Conversely, it has been demonstrated that lanthanide(III) complexes, particularly those having bulky substituent on the tridentate ligands are prone to decoordination of the bulky coordinating parts, especially at low concentrations.[31] On may consider a temperature dependent equilibrium between complexes containing the tridentate ligands and the solvated complex as the suggested mechanism to explain the ratiometric luminescence characteristics as observed for **1**–**5** (Figs. 2a-e). Then, we have checked the stability of the complex at low concentrations by in-situ preparation (i.e., titration analysis) of complex **1** through successive injection of the corresponding tridentate ligand to the tris-β-diketonate Eu^{3+} complex (**9**) at the low concentration (1.0×10^{-5} M) in acetonitrile. The titration analysis revealed that UV/Vis spectral change is almost complete when 1.0 equivalent of the tridentate co-ligand is added (Fig. S1, ESI†), suggesting the binding of the tridentate co-ligand to the tris-β-diketonate Eu^{3+} complex (**9**) is almost stoichiometric even under low concentration conditions. In addition to this, the ratiometric spectral variations in the extremely narrow *f-f* transition bands vary depending on the symmetry (C_S vs C_{2V}) of the β-diketonate ligands (*vide supra*, Table 1; Fig. 2). Thus, we consider the coordination-rearrangement (as described in Scheme 1) as the most probable mechanism to account for the ratiometric luminescence characteristics of **1**–**5**.

Eqn (3) represents relationship between the emission spectrum shape of Eu^{3+} and its radiative lifetime (τ_R),[32] which enables us to estimate radiative lifetimes of the two isomers for **1** using spectral integrations of Fig. 2a. Here, $A_{MD,0}$ represents

$$\frac{1}{\tau_r} = A_{MD,0}\, n^3 \left(\frac{I_{tot}}{I_{MD}}\right) \qquad (3)$$

the spontaneous emission probability at the $^5D_0 \rightarrow {}^7F_1$ transition *in vacuo*, and the value is suggested to be 14.65 s^{-1}.[32] I_{tot}/I_{MD} describes the relative integration ratio of the total area of the Eu^{3+} emission bands to the $^5D_0 \rightarrow {}^7F_1$ band, and n is refractive index of the solvent. The presented analysis indicates the almost same radiative lifetime τ_R = 1.4 ms for the dominant isomers formed at lower and higher temperatures, which implies similar degree of coordination symmetry between the two isomers.

Among the series of nona-coordinated Eu^{3+} complexes, suitable crystals were successfully grown by slow evaporation of acetone solutions of **4** (for the crystallographic data, refer to Table 3).[33] X-ray crystallography analysis determined a coordination arrangement of the three β-diketonate ligands around the Eu^{3+} center (Fig. 6a). Since lanthanide(III) complexes are generally labile, there is not always complete agreement between the crystal and solution structures, especially if such the two solution structures (isomers) are present in the solution equilibrium. We could not emphasize the complete agreement between the crystal and solution structures. However, the crystal structure is informative enough to draw the configuration of nona-coordinated Eu^{III} complexes, considering the proposed mechanism to explain the ratiometric luminescence characteristics of **1**–**5** having unsymmetrical β-diketonate ligands (*vide infra*). The crystal structure revealed that two β-diketonate ligands (A and B) are almost co-planar and the other (C) is in the vertical position (Fig. 6a). The A and B ligands are in the trans position, hence coordination-rearrangement of these ligands results in isomerization of the nona-coordinated Eu^{3+} complex. There are four possible coordination isomers (isomer i-iv) depending on the coordination-rearrangement of the ligands A-C (Figs. 6a and b).[34] One can consider that that the interconversion between more than two isomers, however the ratiometric spectral variations of **1**–**5** with iso-emissive points (Figs. 2a-e) underline the interconversion between the two isomers. The definitive identification of the two complex species in the solution equilibrium could be difficult.

Table 3 Crystallographic parameters and refinement details for complex **4**

Formula sum	$C_{42}H_{29}EuF_9N_3O_{10}$
Formula weight	1058.64
Crystal system	monoclinic
Space group	C 2/c (#15)
a (Å)	31.99(3)
b (Å)	16.708(19)
c (Å)	17.186(19)
α (deg)	90
β (deg)	115.666(10)
γ (deg)	90
V (Å^3)	8279.41(16)
T (K)	173
Z	8
F_{000}	4208.0
ρ calcd (g cm^{-3})	1.699
R1 [I > 2s(I)]	0.0285
wR2 [I > 2s(I)]	0.0635

Solid state emission spectra of **4** were also recorded at various temperatures between 253 and 323 K (Fig. 2j). The splitting patterns of the $^5D_0 \rightarrow {}^7F_1$, $^5D_0 \rightarrow {}^7F_3$ and $^5D_0 \rightarrow {}^7F_4$ transition bands were found to be identical at each temperature, although the relative emission intensity of the $^5D_0 \rightarrow {}^7F_2$ transition band almost doubled on going from 323 to 253 K (Fig. 2j). Since there is insufficient void space for the β-diketonate ligand to rearrange in the solid state, the observed relative intensity change must originate from a local symmetry change of the Eu^{3+} metal centre at the lower temperature. Consequently, the nona-coordinate Eu^{3+} complex having unsymmetrical β-diketonate ligands can also function as a single lanthanide-based ratiometric luminescence thermo-sensor in the solid state.

Conclusions

In conclusion, we have successfully demonstrated that the ligand symmetry of nona-coordinated Eu^{3+} complexes controls the ratiometric luminescence characteristics of these compounds. Coordination-rearrangement of the unsymmetrical β-diketonate ligand around the Eu^{3+} causes isomerization of the nona-coordinated Eu^{3+} complexes, resulting in varying crystal field effects. The two coordination isomers are in a temperature-dependent equilibrium, with one generating intense emission at 612 nm and the other a sharp emission peak at 620 nm. Consequently, the relative intensity ratio changes reversibly as the temperature changes, with distinct iso-emissive points. This phenomenon enables nona-coordinated Eu^{3+} complexes with unsymmetrical β-diketonate ligands (**1**–**5**) to work as lanthanide-based ratiometric luminescence thermo-sensors. The proposed mechanism was validated through experiments with reference Eu^{3+} complexes having symmetrical β-diketonate ligands (**6**–**8**). A new self-calibration method using dual iso-emissive points was also successfully demonstrated, in which self-calibration using the two emission intensities at the iso-emissive points reduces the coefficient of variation (*CV*). The present methodology is not restricted to luminescence thermometry and could potentially be applied to various sensing systems, including mixed lanthanide systems, because ligand symmetry is a basic concept in coordination chemistry. Thus, our findings should be generally applicable to the development of new optical ratiometric systems based on crystal-field symmetry.

Experimental section

General. ^{1}H NMR spectra were measured with JEOL ECZ400S (400 MHz). Chemicals were purchased from Wako Pure Chemical Industries Ltd. and used as received without further purification. (*R*,*R*)-2,6-Bis(4-isopropyl-2-oxazolin-2-yl)pyridine and 2,2':6',2''-terpyridine were obtained from Tokyo Chemical Industry Co., Ltd. (TCI). 4,4,4-Trifluoro-1-(4-furyl)butane-1,3-dione was obtained from Aldrich and 4,4,4-trifluoro-1-(4-phenyl)butane-1,3-dione was obtained from Wako Pure Chemical Industries Ltd. (*R*)-2-(6-(4,5-Dihydrooxazol-2-yl)pyridin-2-yl)-4-isopropyl-4,5-dihydrooxazole was prepared according to a procedure described previously.[35] The emission lifetimes were recorded using FluoroCube (HORIBA, 3000 U-YSP) with the Multi Chanel Scale (MCS) mode. The positive ESI mass spectra of the Eu(III) complexes were measured with mass spectrometers (JEOL AccuTOF CS JMS-T100CS for ESI). The emission and UV-vis absorption spectra of the Eu(III) complexes were measured at various temperature using JASCO FP-6500 and V-660, respectively. The CD spectra of the Eu(III) complexes were measured using JASCO-725.

Crystallography. Suitable crystal of **2** was obtained by slow evaporation of the acetone solution of **2**. Single crystal of **2** was mounted with Dual-Thickness MicroMounts. X-ray diffraction intensity was collected with a Bruker AXS・SMART APEX CCD detector with graphite monochromated Mo Kα radiation at 100 K. All calculations were performed with the APEX3 software.

Synthesis. Tris-β-diketonate Eu^{3+} complexes as precursor complexes were prepared as describe in the literature.[36] The nona-coordinated Eu^{3+} complexes **1–8** were synthesized as follows. Typically, 2,2':6',2''-terpyridine (0.17 mmol) and the corresponding tris-β-diketonate Eu^{3+} complex (0.17 mmol) were dissolved in methanol (30 mL) in flask. The reaction mixture was stirred for overnight at room temperature. After removing the solvent by evaporation, the obtained white powder was dried under vacuum (**4**, yield: 85%). The other nona-coordinated Eu^{3+} complexes complexes were prepared by using the same procedures. Complex **7** was prepared as describe in the literature.[16]

1: ^{1}H NMR (400 MHz, CD_3CN) 18.25 (br, 2H), 13.41 (br, 2H), 8.79–9.04 (m, 5H), 8.45 (br, 2H), 6.05–6.94 (m, 15H), 4.86 (br, 12H), 1.00 (dd, J = 9.6, 6.4 Hz, 2H). HRMS [ESI-MS (positive)]: *m*/*z* calcd. for $C_{37}H_{35}EuF_6N_3O_6$ ([M – L]$^+$), 882.16285; found 882.16191.

2: ^{1}H NMR (400 MHz, CD_3CN) 19.58 (br, 2H), 13.77 (br, 2H), 9.17 (br, 2H), 8.60 (m, 3H), 8.28 (br, 2H), 6.05 (br, 6H), 5.70 (br, 6H), 5.20 (br, 6H), 3.28 (d, J = 5.5 Hz, 3H). HRMS [ESI-MS (positive)]: *m*/*z* calcd. for $C_{33}H_{31}EuF_6N_3O_8$ ([M – L]$^+$), 862.12138; found 862.12039.

3: ^{1}H NMR (400 MHz, CD_3CN) 11.47 (d, J = 7.3 Hz, 2H), 10.22 (t, J = 7.6 Hz, 2H), 8.70 (d, J = 7.3 Hz, 2H), 8.07 (t, J = 7.6 Hz, 1H), 7.88 (d, J = 7.3 Hz, 2H), 6.69–6.86 (m, 9H), 5.85 (br, 6H), 2.89 (br, 2H). HRMS [ESI-MS (positive)]: *m*/*z* calcd for $C_{45}H_{29}EuF_9N_3O_6Na^+$ [M + Na]$^+$: 1054.10226; found 1054.10293.

4: ^{1}H NMR (400 MHz, CD_3CN) 11.51 (d, J = 6.4 Hz, 2H), 10.21 (t, J = 7.0 Hz, 2H), 8.49 (d, J = 6.7 Hz, 2H), 7.81 (t, J = 7.6 Hz, 1H), 7.55 (d, J = 6.7 Hz, 2H), 6.10 (br, 3H), 5.99 (br, 3H), 5.29 (br, 3H), 2.77–2.95 (br, 2H). HRMS [ESI-MS(positive)]: *m*/*z* calcd for $C_{39}H_{23}EuF_9N_3O_9Na^+$ [M + Na]$^+$: 1024.04005; found 1024.03971.

5: ^{1}H NMR (400 MHz, CD_3CN) 11.42 (br, 2H), 10.17 (d, J = 7.3 Hz, 1H), 9.96 (t, J = 7.3 Hz, 1H), 9.83 (br, 1H), 9.47 (br, 1H), 9.32 (d, J = 7.3 Hz, 1H), 8.08 (br, 2H), 7.78 (br, 1H), 7.31 (m, 1H), 5.96–6.96 (m, 15H), 3.29 (d, J = 4.3 Hz, 3H), 2.52 (d, J = 3.1 Hz, 3H). HRMS [ESI-MS (positive)]: *m*/*z* calcd for $C_{44}H_{35}EuF_9N_3O_8Na^+$ [M + Na]$^+$: 1080.13904; found 1080.13760.

6: HRMS [ESI-MS (positive)]: *m*/*z* calcd for $C_{30}H_{14}EuF_{18}N_3O_6Na^+$ [M + Na]$^+$: 1029.97051; found 1029.97026.

8: HRMS [ESI-MS(positive)]: *m*/*z* calcd for $C_{29}H_{20}EuF_{18}N_3O_8Na^+$ [M + Na]$^+$: 10856.00729; found 1056.00899.

Conflicts of interest

There are no conflicts to declare.

Acknowledgements

This research was partly supported by JST-PRESTO "Molecular technology and creation of new functions" (14530027), JSPS

KAKENHI Grant Number JP17H05386 in Scientific Research on Innovative Areas "Coordination Asymmetry" and JP26410094 in Scientific Research (C) as well as the Asahi Glass Foundation.

Notes and references

1 (*a*) C. Görller-Walrand and K. Binnemans, in Handbook on the Physics and Chemistry of Rare Earths, ed. K. A. Gschneidner and L. Eyring, Elsevier, Amsterdam, 1996, vol. 23, p. 121; (*b*) M. C. F. Cunha, H. F. Brito, L. B. Zinner and G. Vicentini and A. B. Nascimento, *Coord. Chem. Rev*., 1992, **119**, 1; (*c*) K. Binnemans, *Coord. Chem. Rev*., 2015, **295**, 1; (*d*) C. C. Bryden and C. N. Rellley, *Anal. Chem*., 1982, **54,** 610; (*e*) G. Vicentini, L. B. Zinner, J. Zukerman-Schpector and K. Zinner, *Coord. Chem. Rev.*, 2000, **196,** 353.
2 Richardson, F. S. *Inorg. Chem*., 1980, **19**, 2806.
3 (*a*) D. G. Smith, B. K. McMahon, R. Pal and D. Parker, *Chem. Commun*., 2012, **48**, 8520; (*b*) B. K. McMahon and D. Parker, *RSC Adv*., 2014, **4**, 37649; (*c*) D. G Smith, R. Pal, and D. Parker, *Chem. Eur. J*., 2012, **18**, 11604; (*d*) G.-L. Law, R. Pal, L. O. Palsson, D. Parker and K.-L. Wong, *Chem. Commun*., 2009, 7321.
4 (*a*) J. Yuasa, T. Ohno, H. Tsumatori, R. Shiba, H. Kamikubo, M. Kataoka, Y. Hasegawa and T. Kawai, *Chem. Commun*., 2013, **49**, 4604; (*b*) J. Yuasa, R. Mukai, Y. Hasegawa and T. Kawai, *Chem. Commun.*, 2014, **50**, 7937; (*c*) Y. Kuramochi, T. Nakagawa, T. Yokoo, J. Yuasa, T. Kawai and Y. Hasegawa, *Dalton Trans*., 2012, **41**, 6634.
5 M. S. Tremblay, M. Halim and D. Sames, *J. Am. Chem. Soc*. 2007, **129**, 7570.
6 (*a*) Y. Cui, F. Zhu, B. Chen and G. Qian, *Chem. Commun*., 2015, **51**, 7420; (*b*) X. Rao, T. Song, J. Gao, Y. Cui Y. Yang, C. Wu, B. Chen and G. Qian, *J. Am. Chem. Soc*., 2013, **135**, 15559.
7 C. D. S. Brites, P. P. Lima, N. J. O. Silva, A. Millan, V. S. Amaral, F. Palacio and L. D. Carlos, *New J. Chem*., 2011, **35**, 1177.
8 D. Ananias, F. A. A. Paz, D. S. Yufit, L. D. Carlos and J. Rocha, *J. Am. Chem. Soc*., 2015, **137**, 3051.
9 (*a*) K. Miyata, Y. Konno, T. Nakanishi, A. Kobayashi, M. Kato, K. Fushimi and Y. Hasegawa, *Angew. Chem., Int. Ed*., 2013, **52**, 6413; (*b*) M. Hatanaka, Y. Hirai, Y. Kitagawa, T. Nakanishi, Y. Hasegawa and K. Morokuma, *Chem. Sci*., 2017, **8**, 423.
10 J. Lehr, M. Tropiano, P. D. Beer, S. Faulkner and J. J. Davis, *Chem. Commun*., 2015, **51**, 15944.
11 J.-W. Ye, J.-M. Lin, Z.-W. Mo, C.-T. He, H.-L. Zhou, J.-P. Zhang and X.-M. Chen, *Inorg. Chem*., 2017, **56**, 4238.
12 (*a*) J.-C. G. Bünzli and C. Piguet, *Chem. Soc. Rev*., 2005, **34**, 1048; (*b*) J.-C. G. Bünzli, *Chem. Rev*., 2010, **110**, 2729.
13 S. V. Eliseeva and J.-C. G. Bünzli, *Chem. Soc. Rev*., 2010, **39**, 189.
14 R. Carr, N. H. Evans and D. Parker, *Chem. Soc. Rev*., 2012, **41**, 7673.
15 F. Zinna and L. Di Bari, *Chirality*, 2015, **27**, 1.
16 J. Yuasa, T. Ohno, K. Miyata, H. Tsumatori, Y. Hasegawa and T. Kawai, *J. Am. Chem. Soc*., 2011, **133,** 9892;
17 (*a*) Y. Okayasu and J. Yuasa, *Mol. Syst. Des. Eng*., 2017, **3**, 66; (*b*) T. Y. Bing, T. Kawai and J. Yuasa, *J. Am. Chem. Soc*. **2018**, *140*, DOI: 10.1021/jacs.7b12663.
18 A. de Bettencourt-Dias, P. S. Barber and S. Bauer, *J. Am. Chem. Soc.,* 2012, **134**, 6987.
19 B. Yan, *Acc. Chem. Res*., 2017, **50**, 2789.
20 L. Li, Y. Zhu, X. Zhou, C. D. S. Brites, D. Ananias, Z. Lin, F. A. A. Paz, J. Rocha, W. Huang and L. D. Carlos, *Adv. Funct. Mater.*, 2016, **26**, 8677.
21 H. S. Peng, M. I. Stich, J. B. Yu, L. N. Sun, L. H. Fischer and O. S. Wolfbeis, *Adv. Mater*., 2010, **22**, 716.
22 D. Ananias, A. D. G. Firmino, R. F. Mendes, F. A. A. Paz, M. Nolasco, L. D. Carlos and J. Rocha, *Chem. Mater*., 2017, **29**, 9547.
23 Y. Zhou, B. Yan and F. Lei, *Chem. Commun*. 2014, **50**, 15235.
24 Y. Cui, R. Song, J. Yu, M. Liu, Z. Wang, C. Wu, Y. Yang, Z. Wang, B. Chen and G. Qian, *Adv. Mater*., 2015, **27**, 1420.
25 X. Liu, S. Akerboom, M. Jong, I. Mutikainen, S. Tanase, A. Meijerink and E. Bouwman, *Inorg. Chem*., 2015, **54**, 11323.
26 Y. Takei, S. Arai, A. Murata, M. Takabayashi, K. Oyama, S. i. Ishiwata, S. Takeoka and M. Suzuki, *ACS Nano*, 2014, **8**, 198.
27 H. Zhang, L. Zhou, J. Wei, Z. Li, P. Lin and S. Du, *J. Mater. Chem*., 2012, **22**, 21210.
28 (*a*) F. Gutierrez, C. Tedeschi, L. Maron, J.-P. Daudey, R. Poteau, J. Azema, P. Tisnes and C. Picard, *Dalton Trans*., 2004, 1334; (*b*) S. Katagiri, Y. Tsukahara, Y. Hasegawa and Y. Wada, *Bull. Chem. Soc. Jpn.*, 2007, **80**, 1492.
29 (*a*) J. Kumar, B. Marydasan, T. Nakashima, T. Kawai and J. Yuasa, *Chem. Commun*., 2016, **52**, 9885; (*b*) J. Yuasa, T. Nakagawa, Y. Kita, A. Kaito and T. Kawai, *Chem. Commun*., 2017, **53**, 6748; (*c*) J. Yuasa, H. Ueno and T. Kawai, *Chem.–Eur. J*., 2014, **20**, 8621; (*d*) Y. Imai, T. Kawai and J. Yuasa, *J. Phys. Chem. A*, 2016, **120**, 4131; *(e)* T. Ogawa, J. Yuasa and T. Kawai, *Angew. Chem. Int. Ed.*, 2010, **49**, 5110; (*f*) Y. Imai, T. Kawai and J. Yuasa, *Chem. Commun*., 2015, **51**, 10103.
30 The tris-unsymmetrical β-diketonate Eu^{3+} complex without a tridentate co-ligand (**9**) exhibits a much shorter emission lifetime (τ = 0.69 ms) compared to the complex with the tridentate ligand (**1**, τ = 0.82 ms).
31 P. Kadjane, L. Charbonnière, F. Camerel, P. P. Lainé and R. Ziessel, *J. Fluoresc*. 2008, **18**, 119.
32 M. H. V. Werts, R. T. F. Jukes and J. W. Verhoeven, *Phys. Chem. Chem. Phys*., 2002, **4**, 1542.
33 It should be noted that the Eu^{3+} complex also exhibits a ratiometric emission change over the temperature range from 253 to 323 K in acetone (Fig. S2, ESI†).
34 Isomers i and iv would be identical if one ignores subtle coordination differences.
35 H. Nishiyama, N. Soeda, T. Naito and Y. Motoyama, *Tetrahedron: Asymmetry*, 1998, **9**, 2865.
36 Y. Hasegawa, S. Tsuruoka, T. Yoshida, H. Kawai, T. Kawai, *J. Phys. Chem. A*, 2008, **112**, 803.

Graphical abstracts

Nona-coordinated europium(III) complexes incorporating unsymmetrical β-diketonate ligands exhibit distinctive ratiometric spectral changes within the extremely narrow *f-f* transition bands in response to temperature changes over the range from 253 to 323 K.